Kinetic Analysis of Simultaneous 2,4-Dinitrotoluene (DNT) and 2,6-DNT Biodegradation in an Aerobic Fluidized-Bed Biofilm Reactor

Barth F. Smets,[1] R. Guy Riefler,[1] Urs Lendenmann,[2]* Jim C. Spain[2]

[1]Environmental Engineering Program, University of Connecticut, 261 Glenbrook Road, U-37, Storrs, Connecticut 06269-2037; telephone: (860)-486-2270; fax: 860-486-2298; e-mail: bsmets@engr.uconn.edu
[2]U.S. Air Force Armstrong Laboratory, AFRL/MLQR, Tyndall AFB, Florida

Received 5 February 1998; accepted 20 November 1998

Abstract: We previously reported on the mineralization of 2,4-dinitrotoluene (2,4-DNT) and 2,6-dinitrotoluene (2,6-DNT) in an aerobic fluidized-bed bioreactor (FBBR) (Lendenmann et al. 1998 *Environ Sci Technol* 32:82–87). The current study examines the kinetics of 2,4-DNT and 2,6-DNT mineralization at increasing loading rates in the FBBR with the goal of obtaining system-independent kinetic parameters. At each steady state, the FBBR was subjected to a set of transient load experiments in which substrate flux in the biofilm and bulk substrate concentrations were measured. The pseudo-steady-state data were used to estimate the biokinetic parameters for 2,4-DNT and 2,6-DNT removal using a mechanistic mathematical biofilm model and a routine that minimized the sum of the squared residuals (RSS). Estimated kinetic parameters varied slightly for each steady-state; retrieved parameters for q_m were 0.83 to 0.98 g DNT/g XCOD d for 2,4-DNT removal and 0.14 to 0.33 g DNT/g XCOD d for 2,6-DNT removal. K_s values for 2,4-DNT removal (0.029 to 0.36 g DNT/m^3) were consistently lower than K_s values for 2,6-DNT removal (0.21 to 0.84 g DNT/m^3). A new approach was introduced to estimate the fundamental biofilm kinetic parameter $S^*_{b,min}$ from steady-state performance information. Values of $S^*_{b,min}$ indicated that the FBBR performance was limited by growth potential. Adequate performance of the examined FBBR technology at higher loading rates will depend on an improvement in the growth potential. The obtained kinetic parameters, q_m, K_s, and $S^*_{b,min}$, can be used to aid in the design of aerobic FBBRs treating waters containing DNT mixtures. © 1999 John Wiley & Sons, Inc. *Biotechnol Bioeng* **63**: 642–653, 1999.

Keywords: DNT; dinitrotoluene; biofilm kinetics; FBBR; parameter estimation

INTRODUCTION

Dinitrotoluenes (DNT) are intermediates in the production of the explosive trinitrotoluene (TNT) and precursors in toluenediisocyanate synthesis used in the manufacturing of polyurethanes (Hartter, 1985). Dinitrotoluenes are formed by the sequential nitration of toluene and the 2,4-DNT and 2,6-DNT isomers typically occur in a 4:1 ratio (Popp and Leonard, 1985). Improper disposal practices associated with TNT manufacturing have resulted in contamination of soils and waters with dinitrotoluenes. Furthermore, DNT-laden waste streams continue to be generated in the manufacturing of explosives and polyurethanes. Both 2,4-DNT and 2,6-DNT exhibit acute toxicity and low-level carcinogenicity and present an environmental health concern (Rickert et al., 1984; Whong and Edwards, 1984), whereas 2,4-DNT is listed as a U.S. EPA priority pollutant (Keith and Telliard, 1979).

Biological treatment can remove DNT from contaminated waste streams. The biotransformation of DNT has been documented under a variety of conditions. Originally observed pathways involved the enzymatic reduction of one or both of the nitrogroups, and intermediates such as nitroso, amino, and azoxy compounds were identified (Liu et al., 1984; McCormick et al., 1978). The electron-withdrawing character of the nitrogroups impedes electrophilic attack by oxygenases of aerobic bacteria (Rieger and Knackmuss, 1995). Nevertheless, oxidative mineralization of 2,4-DNT by pure and mixed cultures has recently been reported (Bausum et al., 1992; Spanggord et al., 1991). The mineralization is concurrent with stoichiometric release of the nitrogroups as NO_2^- (Spanggord et al., 1991). Nitrite release occurs in two steps: the first step is catalysis by the 2,4-DNT dioxygenase, yielding 4-methyl-5-nitrocatechol (4M5NC); subsequently, a monooxygenase catalyzes denitration of 4M5NC to yield 2-hydroxy-5-methylquinone (Haigler et al., 1994). The latter substrate is enzymatically converted and presumably feeds into the Krebs cycle. As a result, 2,4-DNT is completely mineralized without accumulation of intermediates. Several strains that can aerobically mineralize 2,4-DNT as the sole carbon source have since been identified (Spain, 1995). In addition, strains that can use 2,6-DNT as the sole carbon source have recently been isolated (Nishino and Spain, 1996). The initial step in the enzymatic mecha-

* *Present address:* Goldman School of Dental Medicine, Boston University, 700 Albany Street, Boston, MA 02118-2392

Correspondence to: B. Smets

Contract grant sponsors: AFOSR; Strategic Environmental Research and Development Program

CCC 0006-3592/99/060642-12

nism appears very similar to the one observed in the aerobic mineralization of 2,4-DNT (Nishino and Spain, 1996). The advantage of the aerobic mineralization pathways is that no intermediates accumulate. In all nitroreductive pathways, intermediate compounds are formed that may retain toxic properties, be recalcitrant to further mineralization, or require a second-step biological treatment (Cheng et al., 1996, Liu et al., 1984; McCormick et al., 1978; Neumeier et al., 1989; Noguera and Freedman, 1996).

In view of the demonstrated mineralization of 2,4- and 2,6-DNT by aerobic microorganisms, we set out to examine the feasibility of treating a DNT-laden water using an aerobic bioreactor. Because of anticipated low specific growth rates of the DNT-degrading organisms, and because of the relatively low concentrations of DNT in contaminated groundwater (few to 100 ppm), a fluidized-bed bioreactor (FBBR) with sand as the carrier material was chosen. Cells growing on the inert carrier could be protected from washout at low hydraulic retention times, whereas a large volumetric biomass concentration could be retained. We reported earlier on the performance of an aerobic FBBR treating a DNT-laden water (with 2,4-DNT and 2,6-DNT in a 4:1 ratio) at surface loading rates from 36 to 600 mg DNT/m^2 d (Lendenmann et al., 1998). Removals exceeded 99% (98% at highest loading) and 95% (91% at highest loading) for 2,4-DNT and 2,6-DNT, respectively, under steady-state conditions, and complete DNT mineralization was inferred (Lendenmann et al., 1998).

The objective of this study was to examine whether biokinetic parameters for 2,4-DNT and 2,6-DNT removal could be obtained from short-term load-shift experiments (Rittmann et al., 1986). Also, we examined how biokinetic parameters varied as a function of the steady-state surface loading rates. We also wished to improve the reported parameter estimation routine by inclusion of a residuals sum-of-squares minimization routine. Finally, we set out to provide a kinetic explanation for the observation that the FBBR operated in a high load regime — where the effluent substrate concentrations increases rapidly with increases in the surface loading rate — at surprisingly low surface loading rates (Lendenmann et al., 1998).

MATERIALS AND METHODS

Fluidized-Bed Biofilm Reactor Operation and Monitoring

In brief, a 1.5-L water-jacketed fluidized-bed reactor was filled with 0.74 kg of Ottawa sand (30 to 40 mesh) and inoculated with enrichment cultures containing bacteria able to mineralize 2,4-DNT and 2,6-DNT. The reactor was operated at 20°C at a pH of 7 ± 0.1. Aeration was provided by introduction of air to the recirculation line, and dissolved oxygen (DO) concentrations were monitored at the top of the reactor bed and maintained higher than 4.5 mg/L. Recirculation flow rate was set to maintain a flow rate of 1.5 to 1.6 L/min through the bed, resulting in approximately 40% bed expansion. FBBR feed consisted of 2,4 DNT (40 mg/L), 2,6 DNT (10 mg/L), and H_3PO_4 (70 mg/L) in tap water. DO concentration, pH, temperature, bed height, feed flow rate, and recirculation flow rate were measured daily. Samples were removed to measure concentrations of DNT via high-performance liquid chromatography (HPLC). Further details were reported before (Lendenmann et al., 1998).

Biofilm COD and Density Measurements

Samples of sand were removed with a 0.5-mL sampling thimble at two different bed depths. Free water floating on top of the thimble was removed with a KimWipe. The contents of one thimble was transferred to four different aluminum weighing pans and weighed. Pans were dried overnight at 102°C, then reweighed. Approximately 200 μL of deionized H_2O was added to each pan and the sand transferred to one of several COD vials (0 to 150 or 0 to 1500 ppm; Hach, Loveland, CO). Additional H_2O was added to the COD vials to total 2 mL, and vials were held at 150°C for 2 h. The COD concentration was estimated using a HACH spectrophotometer and appropriate potassium phthalate standards. Control COD vials were included that contained clean, acid-washed sand. Vials were opened, the supernatant discarded, and the sand was rinsed with deionized H_2O to remove all reagent. Vials were dried overnight at 102°C. Dried sand was removed and weighed. The biomass COD concentration was calculated as mass of COD/mass of sand. The average mass of evaporated water (W), the total mass of dry sand (M), and the mg XCOD/g sand (X_s) were calculated corresponding to the 0.5-mL sample removed from the bed. The biofilm thickness, L_f, was calculated using the following equation (Rittmann et al., 1986), where a represents the surface area per mass of sand (4.44 m^2/kg) and ρ is the density of water. This equation assumes that the native biofilm mass consists of 99% water;

$$L_f = \frac{W}{0.99aM\rho} \tag{1}$$

Biofilm density, X_f, was calculated by:

$$X_f = \frac{X_s}{aL_f} \tag{2}$$

Load-Shift Experiments

Short-term load-shift experiments were conducted to measure bulk substrate concentrations at different substrate fluxes without altering the physical and kinetic characteristics of the biofilm (Rittmann et al., 1986). Effluent DNT concentrations were measured until they attained steady-state values. Because the biofilm thickness under these conditions is not in true equilibrium with the substrate flux during the load-shift, we refer to these effluent values as pseudo-steady-state concentrations. The FBBR was operated at hydraulic retention times (HRT) of 12, 6, 3, 1.5, and

0.75 h in sequence. For each HRT, steady state was assumed to be achieved when the concentrations of 2,4-DNT and 2,6-DNT varied less than 20% over a period of 3 days. When the FBBR attained steady state, it was subjected to short-term (4-h) shifts in the applied surface loading by varying the feed flow rates. The flow rate through the reactor was instantaneously increased or decreased (from 0.25 to 2.0 times the steady-state flow rate). Flow rates were monitored during the load-shift experiments, and samples were periodically removed from the top of the reactor bed for determination of 2,4-DNT and 2,6-DNT concentrations by HPLC. After 4 h, the reactor was returned to the steady-state flow rate for at least 8 h prior to subjecting the FBBR to another transient load experiment. Transient experiments were performed within a 3-day period at a given steady state.

In Situ Kinetic Parameter Estimation

Data derived from pseudo-steady-state conditions, were used to estimate biokinetic parameters. The flux of substrate into the biofilm, J_{exp}, was calculated by:

$$J_{exp} = \frac{Q(S_o - S_b)}{aM} \tag{3}$$

where, Q is the steady-state flow rate, S_o is the influent concentration, and S_b is the effluent concentation. The average of several pseudo-steady-state effluent concentrations was used as S_b for each load-shift. The substrate concentration at the biofilm/liquid interface, S_s, was calculated by:

$$S_s = S_b - \frac{LJ_{exp}}{D} \tag{4}$$

where, L is the external mass transfer layer thickness and D is the aqueous phase diffusion coefficient for the DNT isomer. The external mass transfer layer thickness was calculated based on the empirical formula (Jennings, 1975):

$$L = \frac{DRe^{0.75}Sc^{0.667}}{5.7\nu} \tag{5}$$

where Re and Sc are the Reynolds and Schmidt numbers, respectively, while ν is the superficial flow velocity. Thus, a pair of S_s and J_{exp} values was determined for each load-shift experiment. S_s and J_{exp} pairs were also determined from the steady-state conditions between each load-shift experiment, providing seven to ten data pairs for each steady-state and DNT isomer.

Extensive theoretical work has been conducted to develop mathematical models which depict the transport and consumption of substrate in biofilms (Rittmann and McCarty, 1980; Wanner and Gujer, 1986). In this investigation, we used a pseudoanalytical expression describing numerical solutions to the biofilm model. Combination of the equations provided by Atkinson and Davies results in three equations to calculate the predicted substrate flux, J_{pr}, as a function of S_s (Atkinson and Davies, 1974):

$$\phi = L_f\left(\frac{q_m X_f}{K_s D_f}\right)^{0.5}\left(1 + \frac{2S_s}{K_s}\right)^{-0.5} \tag{6}$$

$$\xi = \begin{cases} 1 - \left(L_f\left(\dfrac{q_m X_f}{K_s D_f}\right)^{-0.5}\right)\tanh\left(L_f\left(\dfrac{q_m X_f}{K_s D_f}\right)^{0.5}\right)\left(\dfrac{\phi}{\tanh\phi} - 1\right) & \text{if } \phi < 1 \\ \dfrac{1}{\phi} - \left(L_f\left(\dfrac{q_m X_f}{K_s D_f}\right)^{-0.5}\right)\tanh\left(L_f\left(\dfrac{q_m X_f}{K_s D_f}\right)^{0.5}\right)\left(\dfrac{\phi}{\tanh\phi} - 1\right) & \text{if } \phi \geq 1 \end{cases} \tag{7}$$

$$J_{pr} = \frac{\xi L_f S_s q_m X_f}{K_s + S_s} \tag{8}$$

where, q_m is the maximum specific substrate removal rate, K_s is the half-maximum growth coefficient, and D_f is the substrate diffusion coefficient in the biofilm. Most parameters for the model, Q, a, M, X_f, and L_f, were measured experimentally whereas other, L, D, and D_f, were estimated from literature values and correlations. The remaining biokinetic parameters, q_m and K_s, were estimated from the experimental data pairs (S_s, J_{exp}) with a nonlinear unconstrained optimization algorithm. q_m and K_s were varied to minimize the sum of squared residuals (RSS) using the objective function:

$$\min \sum_{i=1}^{n} (J_{exp,i} - J_{pr,i}(q_m, K_s))^2 \tag{9}$$

where, n is the number of data pairs. The conjugate-gradient method using centered difference gradient approximations was used to find a q_m and K_s pair that solves Eq. (9) using both a FORTRAN 77 code and the SOLVER routine in Microsoft EXCEL.

To measure reliability of the parameter estimates, approximate confidence regions were estimated using an F-test (Beck and Arnold, 1977). This method generates 95% confidence contours in the parameter space. The 95% confidence intervals were then taken as the minimum and maximum values on the 95% contour. To examine whether global and not local minima were being retrieved, the optimization routine was started from multiple starting points, and the response surface was generated and examined for multiple minima.

Several statistical techniques were employed to determine the appropriateness of the model for fitting the data at each steady-state HRT. First, four standard diagnostic plots were generated for each DNT isomer at each HRT steady state: (1) J_{pr} versus J_{exp}; (2) a normal probability plot of the standardized residuals, e^*; (3) e^* versus S_s; and (4) e^* versus J_{exp} (Devore, 1987). Standardized residuals were calculated by:

$$e_i^* = \frac{y_i - \hat{y}_i}{s\sqrt{1 - \frac{1}{n} - \frac{(x_i - \bar{x})^2}{\sum_{j=1}^{n}(x_j - \bar{x})^2}}} \quad (10)$$

where y_i is an observed output (for this study $J_{exp,i}$), $\hat{y}_i$ is the model-predicted value ($J_{pr,i}$), x_i is the model input value ($S_{s,i}$), $\bar{x}$ is the mean input value (mean of S_s values for that HRT and DNT isomer), and s is the standard deviation of errors. Likewise, s was approximated by:

$$s^2 = \frac{\sum_{i=1}^{n}(y_i - \hat{y}_i)^2}{n - 2} \quad (11)$$

where $n - 2$ degrees of freedom were used because two parameters were estimated. Normal probability plots were created by ranking the e^* data, determining the percentile value for each ranked e^* [100 $(i - 0.5)/n$], and plotting the e^* values versus the z value of the normal distribution corresponding to the percentile. These plots are effective in revealing model accuracy, model error normality, and model error heteroscedasity. The null hypothesis (H_o) that e^* was normally distributed was tested by comparing the regression value from a linear regression of the normal probability plot against a test statistic (Devore, 1987). In addition, error plots using values from all of the individual models were generated to yield a larger data set. Two additional statistical tests were performed on each model calibration: a paired t-test and a chi-square goodness-of-fit test (Schnoor, 1996). These methods quantitatively test the H_o that the experimental values equal the model-predicted values to a specified level of significance.

Mass Transfer

The relative effect of mass transfer resistance was investigated using the Biot number and K^*. The Biot number, Bi, measures the relative contribution of internal and external mass transfer resistance and was calculated by (Characklis et al., 1990):

$$Bi = \frac{k_L L_f}{D_f} = \frac{DL_f}{D_f L} = \frac{L_f}{0.8L} \quad (12)$$

where k_L is the external mass transfer resistance. The biofilm diffusion coefficient, D_f, was assumed as 0.8 times the aqueous phase diffusion coeffcient, D (Williamson and McCarty, 1976).

K^* captures the relative contribution of the external mass transfer resistance to the internal mass transfer and biokinetic transformation and was calculated as described in (Sáez and Rittmann, 1990):

$$K^* = \frac{D}{L}\sqrt{\frac{K_s}{q_m X_f D_f}} \quad (13)$$

Monte Carlo Simulations

Monte Carlo analysis was conducted to determine whether the parameter estimation scheme retrieved the true parameters and to estimate the accuracy of those estimates when realistic error in the parameters and model input was considered. For these simulations, D, D_f, L, S_o, a, M, and Q were assumed without error, whereas known errors were associated with S_b, L_f, and X_f. The steps used for Monte Carlo simulations were as follows. First, the "true" biofilm parameters were selected, and eight S_b values were computed, representing the "true" conditions in the reactor. Next, a realization was created by adding normally distributed error to L_f and X_f and the eight S_b values to create "measured" values that included typical experimental error. Pairs of S_s and J_{exp} values were calculated using Eqs. (3) and (4) with the "measured" values. The parameters, q_m and K_s, were estimated using the model with the "measured" S_s, J_{exp}, X_f, and L_f values. Two ensembles of 1000 realizations each were created, one for each DNT isomer. Chi-square goodness-of-fit tests were conducted to determine the distribution of each ensemble of parameter estimates, and the mean and standard deviations were estimated. Errors in L_f, X_f, and S_b were assumed to be normally distributed, uncorrelated, and with means of zero. Standard deviations for L_f, X_f, and S_b were calculated from replicate experimental measurements.

RESULTS

Biofilm Thickness

The biofilm concentrations (per mass of sand) measured at each steady state were reported previously (Lendenmann et al., 1998). The biofilm concentration increased with increases in the applied substrate loading; proteinaceous matter constituted 27% (with a standard deviation of 4%) of the biomass COD. Here, we report the biofilm density and biofilm thickness that were determined during the last three steady states (i.e., at HRTs of 3, 1.5, and 0.75 h; Table I). The biofilm thickness, estimated from weight loss upon drying using Eq. (1), varied little with increased surface loading rates, whereas the biofilm density increased from 8200 g/m^3 (±900 g/m^3) to 13,400 g/m^3 (±970 g/m^3) to

Table I. Steady-state biofilm concentration, density, and thickness.

HRT (h)	COD[a] (mg XCOD/g sand)	L_f (μm)	Density (g XCOD/m^3)
12	0.85 ± 0.14	55[b] NA	3500 NA
6	0.95 ± 0.03	55[b] NA	3900 NA
3	2.22 ± 0.11	55 ± 2	8200 ± 910
1.5	3.11 ± 0.07	53 ± 3	13,400 ± 970
0.75	5.03 ± 0.77	58 ± 11	19,600 ± 820

[a]Data from Lendenmann et al. (1998).

[b]Thickness estimated as the average thickness observed at all other steady states.

19,600 g/m^3 (±820 g/m^3) with subsequent twofold decreases in HRT.

Parameter Estimation

Profiles from the load-shift experiments associated with a 1.5-h HRT have been illustrated previously (Lendenmann et al., 1998). Data presented here refer to the 6-h HRT (Fig. 1). The feed flow rates were changed at time 0 to achieve nominal HRTs of 24, 12, 3, and 1.5 h. The response in effluent concentrations was very rapid. When the hydraulic retention time was decreased (increasing the applied surface loading), the effluent concentrations for 2,4-DNT and 2,6-DNT increased rapidly. The converse was observed for increases in the HRT. In most cases, new pseudo-steady-state DNT values were obtained. For the highest flow rate shifts, no pseudo-steady-state was attained for 2,6-DNT. The 2,6-DNT concentrations continued to increase because the maximum removal rates were exceeded. Load-shift experiments that did not attain pseudo-steady-state were not used in subsequent kinetic parameter estimation. The average effluent concentrations during the pseudo-steady-state were calculated, and used to derive (S_s, J_{exp}) data pairs. All load-shift experiments at all steady-states followed the expected profiles of decreasing S_s values with decreasing J_{exp} values, and a sharp increase of S_s beyond a critical value of J_{exp} reflective of the onset of high load conditions (Figs. 2 and 3).

Parameter estimates at each steady-state are listed in Table II and the best-fit profiles are plotted with the experimental data in Figures 2 and 3. The response surface for nine of the ten data sets exhibited a minimum, indicating an optimal data fit with the exception of 2,4-DNT at an HRT of 3 h (Fig. 2c). Analysis of the response surface for this data set indicated a minimum with $K_s \leq 0$, which is physically impossible and numerically incalculable. Problems with dissolved oxygen and pH control experienced during these load-shift experiments are probable explanations for the resulting poor experimental data. In addition, upper bounds for the 95% confidence interval could not be determined for 2,6-DNT removal at an HRT of 12 h because the 95% confidence contour was not closed. The cause of this was the scatter in the two data points with highest S_s values (Fig. 3a). As long as the fit was between these widely spaced points, the change in RSS was minimal, allowing very large parameter values while still fitting the data. Although estimated parameters varied from steady-state to steady-state, for nearly all of the parameters for each compound, the

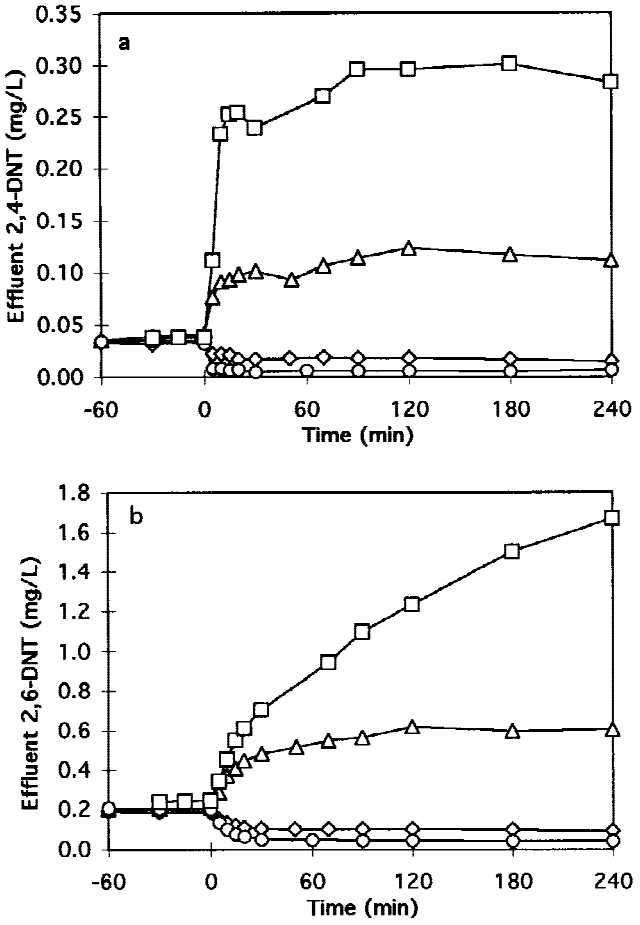

Figure 1. Effluent concentrations of 2,4-DNT (a) and 2,6-DNT (b) during load-shift experiments for the 6-h HRT steady state. The steady-state flow rate was 240 mL/h. Flow rates during the shift were 58 (○), 128 (◇), 480 (△), and 700 (□) mL/h. These correspond to nominal HRTs of 24 (○), 12 (◇), 3 (△), and 1.5 (□) h.

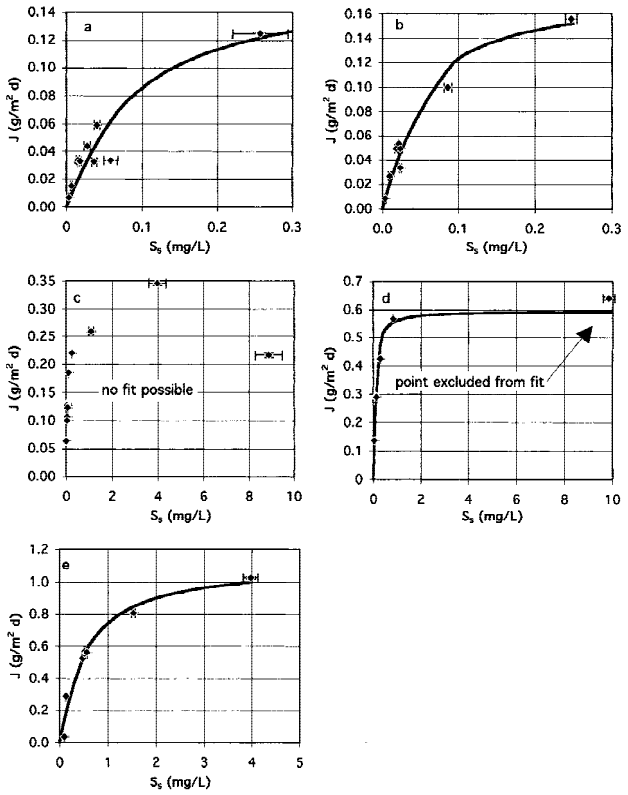

Figure 2. J_{exp} versus S_s and model best fits for 2,4-DNT experiments. Error bars indicate ±1 standard deviation. Panels depict: (a) HRT = 12 h; (b) HRT = 6 h; (c) HRT = 3 h; (d) HRT = 1.5 h; (e) HRT = 0.75 h.

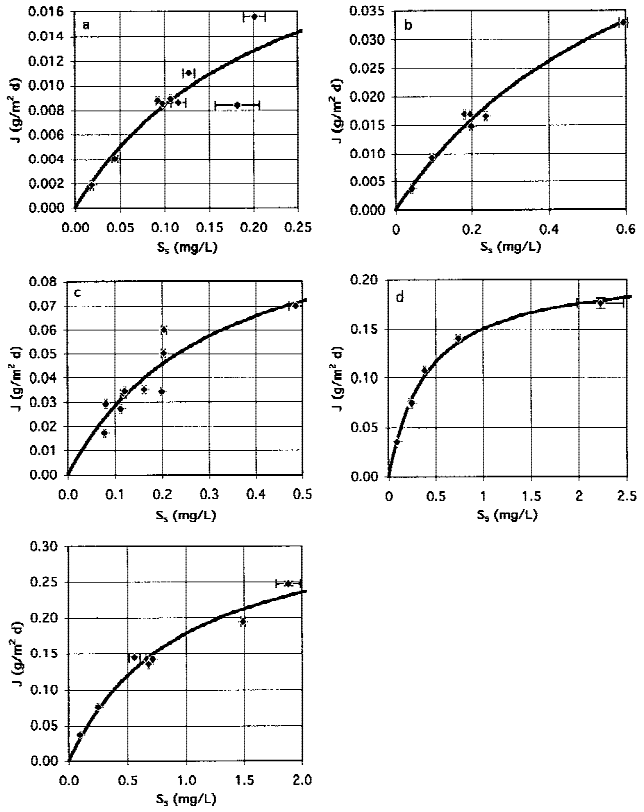

Figure 3. J_{exp} versus S_s and model best fits for 2,6-DNT experiments. Error bars indicate ±1 standard deviation. Panels depict: (a) HRT = 12 h; (b) HRT = 6 h; (c) HRT = 3 h; (d) HRT = 1.5 h; (e) HRT = 0.75 h.

estimated 95% confidence intervals overlapped substantially. However, the estimated K_s value for 2,4-DNT at an HRT of 0.75 h was an order of magnitude higher than the other estimates, and appeared significantly different from the estimate at an HRT of 1.5 h. Differences in biodegradation kinetics for the two DNT isomers were also evident. The maximum specific removal rate (expressed per total biomass COD) was higher for 2,4-DNT than for 2,6-DNT. It also appeared that the affinity for 2,4-DNT was higher (i.e., the K_s value was lower) than for 2,6-DNT, although this is statistically less defensible because of the large confidence intervals for K_s estimates. The lower affinity for 2,6-DNT removal was in agreement with the higher 2,6-DNT effluent concentrations measured during steady-state FBBR operation (Lendenmann et al., 1998).

The estimation routine was repeated for several different initial estimates of q_m and K_s. The routine consistently converged to the same final parameter estimates from different initial (q_m, K_s) estimates, indicating the presence of a single global minimum. Subsequently, response surfaces were examined which confirmed that global rather than local minima were attained during the parameter estimation routine. Figure 4 shows the response surface (RSS) for the parameter estimation for 2,6-DNT at an HRT of 1.5 h. The surface changed smoothly with clearly only one minimum within the space tested. The shape of the response surface at the minimum suggests some correlation between both estimated parameters.

Model fits were examined by a series of four diagnostic plots for each data set individually (data not shown) and for all data sets together (Fig. 5). Linear regression of the fitted versus experimental substrate flux yielded regression coefficients, R^2, very close to 1.00, indicating a good fit of all of the data (Table III, Fig. 5a). Three of the individual data sets had fairly low R^2 values (2,4-DNT at HRT of 12 h, 2,6-DNT at HRTs of 12 and 3 h), and parameter estimates from these data sets had correspondingly the largest confidence intervals (Table II). The null hypothesis that the standardized residuals were normally distributed could not be rejected at a high level of significance for all but two of the data sets (2,4-DNT at HRTs of 12 and 1.5 h, Table III). Standardized error plots showed no obvious pattern for individual or combined data plots (Fig. 5c,d) confirming that the errors did not change with the magnitude of the variables. The data set for 2,4-DNT at an HRT of 1.5 h contained one data point with a standardized residual of 9.5 (Fig. 2d), which was deemed an outlier and not used in parameter estimation for this data set (Bard, 1974). Finally, the null hypothesis that the model values equaled the measured values could not be rejected at high levels of confidence using both paired *t*-tests and chi-square goodness-of-fit tests for all data sets (Table III).

We evaluated whether biokinetic parameters could be estimated for the biofilm without the load-shift experiments, using only steady-state data from the five HRTs. This estimation resulted in one set of average biokinetic parameters for all steady states. Four to six steady-state (S_s, J_{exp}) data pairs were derived from each HRT and kinetic parameters were estimated for the entire data set. The appropriate values for biofilm thickness and densities were used for each HRT (Table I). The resulting set of q_m and K_s estimates for 2,4-DNT and 2,6-DNT were different from the estimates determined by the load-shift experiments. The largest difference was observed in the K_s estimates, where substantially smaller estimates were retrieved from the steady-state data (Table II).

Mass Transfer

Using the Wilke–Chang equation, aqueous phase diffusion coefficients, *D*, for 2,4-DNT and 2,6-DNT were calculated as 6.35×10^{-10} m^2/s (Welty et al., 1984). The mass transfer layer thickness, *L*, was calculated as 16.4 μm using Eq. (5) and remained constant throughout FBBR operation, because particle dimensions, superficial velocity, and bed expansion varied little. The relative contributions of external processes and internal processes was evaluated with two dimensionless parameters. The Biot number, *Bi*, was calculated at 4.2 using Eq. (12) and an average L_f of 55 μm. This *Bi* reveals that the mass transfer resistance is largely manifested inside the biofilm due to the high recycle ratio and a *Re* value of 30. *K** values were computed using Eq. (13) and ranged between 4.3 and 10.2 for 2,6-DNT, and between 0.8 and 2.1

Table II. Best-fit kinetic parameters for 2,4-DNT and 2,6-DNT removal at different steady states.

HRT (h)	q_m (g DNT/g XCOD d)	K_s (g DNT/m^3)	n	RSS	95% confidence interval for q_m	95% confidence interval for K_s
2,4-DNT						
12	0.84	0.065	10	0.0017	0.42–2.87	0.011–0.61
6	0.83	0.029	8	0.00071	0.58–1.23	0.008–0.97
3	NA	NA	NA	NA	NA	NA
1.5	0.85	0.038	7	0.0028	0.70–1.01	0.008–0.083
0.75	0.98	0.36	8	0.025	0.77–1.25	0.16–0.73
SS	0.49	0.0012	23	0.017	0.46–0.54	<0–0.014
2,6-DNT						
12	0.14	0.21	9	0.0000025	0.054–∞	0.020–∞
6	0.33	0.67	7	0.0000096	0.20–0.64	0.35–1.63
3	0.23	0.27	10	0.00044	0.12–0.64	0.07–1.22
1.5	0.30	0.37	8	0.0000087	0.28–0.33	0.30–0.45
0.75	0.30	0.84	8	0.0010	0.22–0.48	0.42–1.99
SS	0.15	0.13	23	0.00075	0.14–0.17	0.078–0.19

NA, the model could not be fit to this data set; SS, using all the steady-state data for the five HRTs but no load-shift data.

for 2,4-DNT. Large values of K^* (on the order of ≥ 1) also indicate that external mass transfer resistance had little effect on overall process performance.

Monte Carlo Simulations

To examine the retrievability of the biokinetic parameters, Monte Carlo simulations were performed using synthetic (S_s, J_{exp}) data sets generated with typical measurement error applied to S_b, X_f, and L_f. Computed standard deviations for S_b measurements were 0.0226 mg/L and 0.0146 mg/L for 2,4-DNT and 2,6-DNT, respectively, and 3.84×10^{-6} m and 950 g XCOD/m^3 for L_f and X_f measurements, respectively. With these values, random error was incorporated into two ensembles of 1000 realizations each. One ensemble was based on estimated parameters for 2,4-DNT removal at an HRT of 6 h, and the other ensemble was based on estimated parameters for 2,6-DNT removal at an HRT of 1.5 h. Results of the Monte Carlo runs are shown in Table IV. The parameter estimation routine retrieved best-fit parameters that were very close to the true value. Best-fit estimates for q_m and K_s were within 1.0% to 2.1% and 2.7% to 5.9% of the true value, respectively. The q_m and K_s distributions for the two ensembles failed to fit either the normal or lognormal distributions using chi-square goodness-of-fit tests.

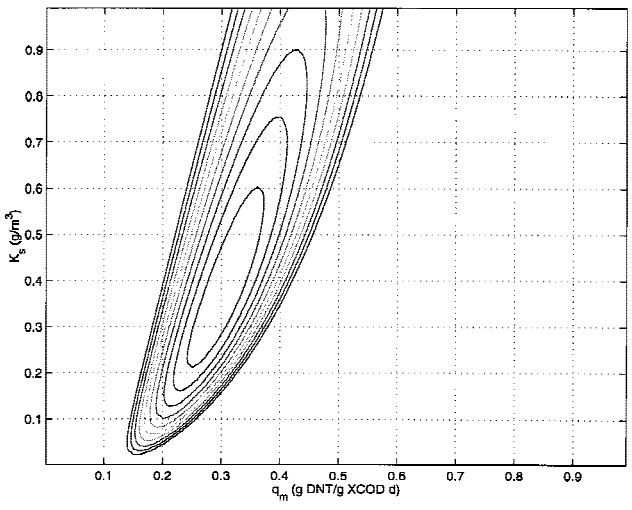

Figure 4. Response surface (RSS) for the parameter estimation of 2,6-DNT at an HRT of 1.5 h. Contours for RSS values of 0.001 increments from 0.001 to 0.01 are shown.

$S^*_{b,min}$ Calculation

Examination of curves of S_b versus J_{exp} (Lendenmann et al., 1998) indicated that the FBBR operated in a high load region, notwithstanding the fairly small applied flux. The maximum steady-state fluxes were approximately $J_{exp} =$

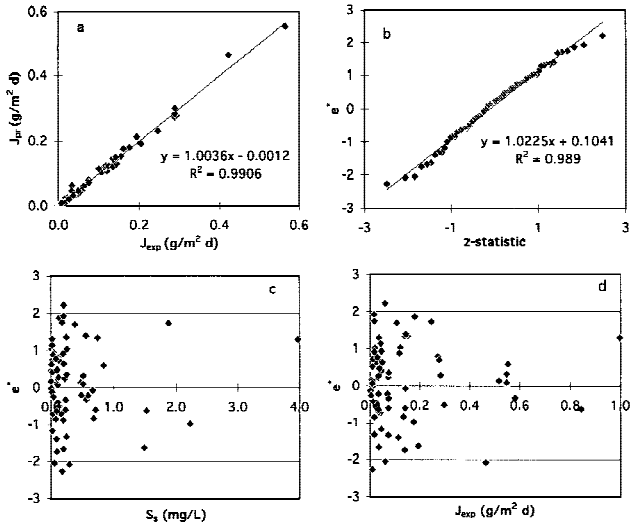

Figure 5. Plots to assess model validity. Data points from all 2,4-DNT and 2,6-DNT experiments for which fitted parameters were obtained are plotted together. Panels depict: (a) J_{pr} versus J_{exp}; (b) normal probability plot of standardized residuals (e^*); (c) e^* versus S_s; (d) e^* versus J_{exp}.

Table III. Statistical tests verifying model appropriateness.

HRT (h)	n	R^2 of J_{pr} vs. J_{exp}	Normality test ($\alpha = 0.05$)	Paired t-test ($\alpha = 0.05$)	Chi-square goodness-of-fit ($\alpha = 0.05$)
2,4-DNT					
12	10	0.8496	Reject	Accept	Accept
6	8	0.9591	Accept	Accept	Accept
3	NA	NA	NA	NA	NA
1.5	7	0.9795	Reject	Accept	Accept
0.75	8	0.9596	Accept	Accept	Accept
SS	23	0.9798	Accept	Accept	Accept
2,6-DNT					
12	9	0.7954	Accept	Accept	Accept
6	7	0.9806	Accept	Accept	Accept
3	10	0.8108	Accept	Accept	Accept
1.5	8	0.9941	Accept	Accept	Accept
0.75	8	0.9659	Accept	Accept	Accept
SS	23	0.9875	Accept	Accept	Accept
All data combined					
	75	0.9906	Accept	Accept	Accept

NA, the model could not be fit to this data set; SS, using all the steady-state data for the five HRTs but no load shift data.

0.45 g 2,4-DNT/m^{2}d and 0.15 g 2,6-DNT/m^{2}d. The fundamental parameter that captures biofilm kinetic behavior is the dimensionless parameter $S^*_{b,min}$ (Sáez and Rittmann, 1988). $S^*_{b,min}$ measures the relative importance of biomass growth versus biomass loss by decay and detachment. Large values of $S^*_{b,min}$ ($\gg 1$) indicate that biomass growth is not much larger than biofilm loss, termed low growth potential. Small values of $S^*_{b,min}$ ($\ll 1$), on the other hand, suggest a high net growth relative to loss, termed high growth potential. $S^*_{b,min}$ is defined as $S_{b,min}/K_s$, wherein:

$$S_{b,min} = \frac{K_s b'}{Yq_m - b'} \tag{14}$$

where b' is the first order biofilm decay coefficient which sums the effects of endogenous biofilm decay and biofilm loss by shear and Y is the bacterial growth yield (Sáez and Rittmann, 1988). After rearrangement $S^*_{b,min}$ becomes:

$$S^*_{b,min} = \frac{1}{\frac{Yq_m}{b'} - 1} \tag{15}$$

Although observed biofilm growth yields and shear loss rates were calculated (Lendenmann et al., 1998), the experimental data did not allow calculation of Y and b' values. However, the ratio of Y/b' could be calculated by recognition of the following equality during steady-state biofilm operation (Sáez and Rittmann, 1988):

$$YJ_{exp} = b' X_f L_f \tag{16}$$

Thus, $S^*_{b,min}$ can be written as:

$$S^*_{b,min} = \frac{1}{\frac{X_f L_f q_m}{J_{exp}} - 1} \tag{17}$$

The $X_f L_f$ term represents the amount of biomass per unit surface area in the FBBR, which can be calculated from the reported values of biofilm mass per unit sand (Lendenmann et al., 1998) with the known specific surface area of the carrier sand. Large values of $S^*_{b,min}$ indicate that the specific biofilm growth rate is largely offset by its specific decay rate, while low $S^*_{b,min}$ values indicate biofilms with high growth potentials. $S^*_{b,min}$ values were calculated for each

Table IV. Results from the Monte Carlo analysis.

	2,4-DNT		2,6-DNT	
	q_m (g DNT/g XCOD d)	K_s (g DNT/m^3)	q_m (g DNT/g XCOD d)	K_s (g DNT/m^3)
True value	0.828	0.0287	0.300	0.366
Mean estimate	0.845	0.0304	0.303	0.376
Percent error	2.1%	5.9%	1.0%	2.7%
SD of estimate	0.137	0.0119	0.0165	0.0243
CV of estimate	0.162	0.391	0.0545	0.0646

SD, standard deviation; CV, coefficient of variation.

individual steady-state and are reported in Table V. Values of $S^*_{b,min}$ (≈0.5) reveal that the specific growth rate exceeds the total first-order biofilm decay coefficient by a factor of only 3 [see Eq. (15)], suggesting a limitation on the growth potential of the microorganism in the system.

DISCUSSION

The results reported here demonstrate that existing biofilm models and experimental techniques are adequate for analysis and interpretation of simultaneous 2,4-DNT and 2,6-DNT removal in an aerobic fluidized-bed biofilm reactor. Biomass concentrations per unit reactor volume were relatively small as a result of the low loading rates and the small specific surface area of the sand particles. Biofilm thickness measurements, which were performed at the three highest surface loading rates, revealed small variations in the biofilm thickness, but increases in the biofilm density indicated that the biofilm grew more compact with increased loading rates. Typically the opposite has been observed — development of thicker, but less dense, biofilms with increasing loading rates (Shieh and Keenan, 1986). Such density reduction may constitute a mechanism to maximize substrate consumption rates at increasing loading rates due to concomitant reductions in biofilm diffusional resistance (Tanyolaç and Beyenal, 1996). Liu (1997) however, recently measured nitrifying biofilms with very small active thickness (≈20 μm), and reported density increases with increased loading rates. Possibly, at small biofilm thickness, increased loading in combination with the relatively high shear applied ($Re = 30$) causes an increase, rather than decrease of biofilm density.

The FBBR responded very rapidly to short-term shifts in the loading rates, and new pseudo-steady-state values were typically obtained within 1 h after upshifts and within 5 to 10 min after downshifts. The load-shift experiments provided a mechanism to estimate the biokinetic parameters of the biofilm in situ, and without destruction of the biofilm architecture. Sets of pseudo-steady-state data at individual steady states were successfully fit using a mechanistic biofilm model (Atkinson and Davies, 1974). The method applied here used a residual error minimization routine, rather than the visual optimization proposed earlier (Rittmann et al., 1986). Our approach improved confidence in the parameter sets, and allowed us to confirm that parameter estimates were unique and reflective of the global optimum. Diagnostic plots and tests indicated that, except for a few cases, the model served as a good depiction of the experimental data. Experimental and fitted substrate flux values matched closely (Fig. 5a), whereas the standardized residual error behaved normally (Fig. 5b), and was homoscedastic with a mean value of zero in both variables (Fig. 5c,d). Conversely, this analysis indicates that the parameters retrieved by the estimation routines are reliable. In addition, these tests have helped to validate the Gauss–Markov conditions implicitly assumed in least-squares analysis: (1) the expected value for the model or sample error is zero; (2) the samples are not heteroscedastic (variance of error is constant for all samples); and (3) the sample values are uncorrelated (Sen and Muni, 1990). Our results indicate with high probability that the first and second condition were met, whereas the technique employed [different load-shifts for each (S_s, J_{exp}) data pair] favored the third condition that sample values are uncorrelated.

Table V. Estimation of $S^*_{b,min}$ at different steady states.

HRT (h)	2,4-DNT	2,6-DNT
12	0.254	0.471
6	0.350	0.299
3	—	0.451
1.5	0.925	0.537
0.75	0.983	0.703
Average	0.63 (±0.38)	0.49 (±0.15)

Monte Carlo analyses, employing realistic estimates of experimental error, indicated that the estimation routine was able to retrieve true kinetic parameters with satisfactory accuracy (<6% difference, Table V). Estimates from 2,6-DNT experiments were more accurate than from the 2,4-DNT experiments as a result of the smaller error in S_b measurements. In addition, there was less variability in the 2,6-DNT results as evidenced by the coefficient of variation which was an order of magnitude lower than for 2,4-DNT. For 2,4-DNT, there was much more variability in K_s (coefficient of variation = 0.391) than in q_m (coefficient of variation = 0.162), whereas, for 2,6-DNT, the variability was similar for both parameters. Overall, the results indicate that, on average, the parameter estimation method can obtain accurate parameter estimates, although an average of several replicates may be necessary to overcome variability in the measurements.

From the RSS response surface, a correlation between q_m and K_s estimates was observed (Fig. 4). Such q_m/K_s correlation is commonly observed in many suspended and attached growth kinetic assays where Monod parameters are estimated (Holmberg, 1982; Lobry and Flandrois, 1991; Riefler et al., 1998; Robinson and Tiedje, 1983; Van Rolleghem et al., 1995). The confidence regions around the best-fit (q_m, K_s) parameters were quite large (Table II), notwithstanding the sharp definition of the global optimum. The large confidence regions could be improved by performing more load-shift experiments at each steady-state.

The kinetic parameters estimated at individual HRTs differed little, except for the K_s value estimated for 2,4-DNT removal at the shortest HRT (Table II). This consistency was unexpected, as it is well known that culture history and reactor operating conditions can dramatically impact the biokinetic parameters measured from a microbial culture (Grady et al., 1996). For example, ongoing continuous cultivation of pure cultures tends to result in expression of increased substrate affinities (Höfle, 1983; Rutgers et al., 1987), whereas cultivation at higher loading rates tends to result in expression of higher specific substrate removal

rates (Daigger and Grady, 1982; Sokol, 1987, 1988). Continuous cultivation of mixed cultures, on the other hand, is believed to cause the selective enrichment of organisms with high-affinity substrate uptake systems (Chiu et al., 1972; Dykhuizen and Hartl, 1983). The limited variation in kinetic parameter values at different HRTs suggests that the overall physiological states of the biofilm bacterial members at different HRTs were very similar and that parameters measured using the pseudo-steady-state technique at one steady-state HRT can probably be used to predict performance at other HRTs (Grady et al., 1996). The high K_s value measured for 2,4-DNT removal at the shortest HRT may be indicative of a physiological change consistent with the expression of low affinity enzymes under high load conditions (Grady et al., 1996). A good fit to all steady-state reactor data was found (i.e., without load-shift pseudo-steady-states) over the range of HRTs using one global set of biokinetic parameters (Tables II and III). The biokinetic parameters, however, were different from those found using the pseudo steady-state approach method. Because the steady-state-derived parameters are an average of the biofilm behavior throughout its operation, a closer agreement between these parameters and those obtained at individual HRTs would be expected. If the steady-state parameters are considered reflective of the true average biokinetic behavior of the system, the question remains why K_s estimates at individual HRTs were higher. One cause may be related to the rapid increases in concentration of DNT isomers during load upshifts. In separate experiments with 2,4-DNT- and 2,6-DNT-mineralizing bacterial cultures, we observed that DNT isomers at higher concentrations inhibit their own removal, although such inhibition occurs only above concentrations of several milligrams per liter. For 2,4-DNT removal, this inhibition is probably due to the transient accumulation of 4-methyl-5 nitrocatechol (MNC), the first transformation product of 2,4-DNT, which inhibits the MNC monooxygenase in a self-inhibitory mode above approximately 1 mg/L (Haigler et al., 1996). Although, no free methylnitrocatechols were measured during the transient load-shift experiments that attained steady state, such accumulation may have occurred intracellularly, and could cause the higher K_s estimates due to an apparent decrease in substrate affinity at increasing concentrations of a self-inhibitory substrate.

The best-fit kinetic parameters consistently revealed higher maximum specific removal rates for 2,4-DNT than for 2,6-DNT (Table II). This is potentially an artifact of the way the biomass concentrations are measured. The biofilm kinetic parameters are expressed per unit of total biofilm biomass. It has previously been assumed and shown that the fraction of the biomass in a given system capable of degrading a particular target compound is proportional to the fraction of the energy in the feed contributed by that compound (Blackburn et al., 1987; Blok, 1994). Thus, if it is assumed that 2,4-DNT mineralization and 2,6-DNT mineralization are performed by different organisms with similar growth yields, the DNT degrading biomass would consist of 80% 2,4-DNT degraders and 20% 2,6-DNT degraders. Even if 2,4-DNT and 2,6-DNT were degraded in part by the same organisms, it is conceivable that the fraction of catalytic activity involved in the mineralization of each DNT isomer is directly related to their influent concentration. Therefore, to normalize the kinetic parameters per unit of actively degrading biomass, the parameters for 2,4-DNT degradation must be divided by 0.8 and the parameters for 2,6-DNT must be divided by 0.2. This brings the maximum specific removal rates for 2,4-DNT and 2,6-DNT in much closer agreement at each steady state, with the maximum specific removal rates for 2,6-DNT slightly higher than those for 2,4-DNT. Although we assumed no interaction between the mineralization of the DNT isomers, the isolation of some simultaneous 2,4-DNT and 2,6-DNT degraders (Nishino, personal communication) suggests an alternative interpretation that both isomers are consumed as perfectly substitutable substrates for which several kinetic models have been proposed (Egli et al., 1993).

As reported before, the kinetic assay we employed allowed measurement of very low K_s values (Rittmann et al., 1986). The measured K_s values for 2,4-DNT were in agreement with effluent 2,4-DNT concentrations attainable under steady-state operations (Lendenmann et al., 1998). In other assays to estimate biofilm kinetic parameters, much larger K_s values have been reported (Cao and Alaerts, 1995; Nguyen and Shieh, 1995; Zhang and Huck, 1996). Although these differences may be inherent to the different microbial systems studied, the disturbances applied during the kinetic assay and the fact that mass transfer is often not explicitly accounted for in the kinetic expressions employed likely contribute to the measurement of large K_s values. 2,6-DNT removal is, however, characterized by larger K_s values than for 2,4-DNT removal, which indicates that removal of 2,6-DNT to low concentration demands lower loading rates than the removal of 2,4-DNT.

A new approach to estimate the biofilm fundamental parameters, $S^*_{b,min}$, based on steady-state biofilm information, was introduced. Although most parameters in the original definition of $S^*_{b,min}$ can be estimated from influent and effluent analysis, large uncertainty resides in the value of the endogenous decay coefficient, b', which is typically not measured. Computed values of $S^*_{b,min}$ may, therefore, be in error because of an assumed value for b'. The proposed method to calculate $S^*_{b,min}$ uses only steady-state information on biofilm performance, such as the biomass density per unit surface area, the steady-state biofilm flux, and the maximum specific removal rate (estimated through extant analysis). The computed values of $S^*_{b,min}$ revealed that the FBBR may be limited by the growth potential of the microorganisms in the system. For comparison, an $S^*_{b,min}$ value of 0.17 was reported for autotrophic nitrification, which is typically considered a very slow microbial process (Rittmann, 1994). Further improvement to the aerobic FBBR technology for DNT removal would hinge on increases in the growth potential resulting in smaller values of $S^*_{b,min}$. Growth potential increases must involve the increase in Yq_m

or decrease in b'. Conditions should therefore be sought to increase the yield coefficient, improve the maximum specific removal rate, and decrease the endogenous decay rate.

In addition to revealing the existence of growth limitation, $S^*_{b,min}$ values, in concordance with the kinetic parameter estimates, biofilm densities, and external mass transfer layer information, can be used to predict effluent DNT concentrations as a function of applied surface loading rates. We performed biofilm reactor design calculations, based on pseudoanalytical solutions for steady-state biofilms at any biofilm thickness, using the range of estimated kinetic parameters for DNT mineralization (Health et al., 1991). The loading curve can be used to estimate the required applied surface loading rate (≈substrate flux) to attain a target maximum 2,4-DNT and 2,6-DNT effluent concentration. If the system flow rate and influent concentrations are known, the FBBR can be sized to contain the required surface area for biofilm growth.

In conclusion, an existing biofilm kinetic model proved adequate in describing the simultaneous removal of 2,4-DNT and 2,6-DNT during load-shift experiments in an aerobic fluidized-bed bioreactor. Statistical diagnostic plots confirmed that the model provided an appropriate fit to the experimental data. Monte Carlo analysis revealed that the parameter estimation routine, using a residual error minimization approach, was robust. Kinetic parameters reflective of oligotrophic conditions were obtained. External mass transfer resistance proved to have a negligible effect in overall reactor performance. The biofilm density increased with increased applied loading, while the biofilm thickness remained fairly constant. An estimation of the biofilm kinetic parameter, $S^*_{b,min}$, suggested that the biofilm performance was limited by its growth potential, and we suggest a more detailed examination of factors impacting the growth potential could be used to improve reactor performance.

B.F.S. thanks John V. Accashian for assistance in initial development of the parameter estimation routine and comments on the manuscript version of this work. The experimental part of this work was performed while B.F.S. was a Air Force Office of Scientific Research Faculty Research Associate and Urs Lendenmann was a National Research Council Associate at the USAF/Armstrong Laboratory.

NOMENCLATURE

a	surface area per unit mass of sand (L^2/M)
b'	first-order biofilm decay and detachment coefficient ($1/t$)
Bi	Biot number
D	aqueous phase diffusion coefficient (L^2/t)
D_f	biofilm phase diffusion coefficient (L^2/t)
e^*	standardized residual
J_{exp}	flux of substrate into biofilm measured in reactor (≈applied surface loading) ($M/L^2\ t$)
J_{pr}	flux of substrate into biofilm as predicted by model ($M/L^2\ t$)
K^*	contribution of external mass transfer resistance to biofilm performance
k_L	external mass transfer resistance (L/t)
K_s	half-maximum growth coefficient (M/L^3)
L	external mass transfer layer thickness (L)
L_f	biofilm thickness (L)
M	total mass of dry sand in reactor (M)
n	number of data pairs used for each parameter estimation
Q	steady-state flow rate through reactor (L^3/t)
q_m	maximum specific substrate removal rate ($M/M\ t$)
Re	Reynolds number
Sc	Schmidt number
S_b	bulk liquid and effluent substrate concentration (M/L^3)
$S_{b,min}$	minimum S_b to maintain a steady-state biofilm (M/L^3)
$S^*_{b,min}$	unitless $S_{b,min}$ ($S_{b,min}/K_s$)
S_o	substrate concentration of the reactor influent (M/L^3)
S_s	substrate concentration at the biofilm/external mass transfer layer interface (M/L^3)
W	mass of evaporated water from biomass sample (M)
X_f	biofilm bacterial density (M/L^3)
X_s	biomass per unit mass of sand (M/M)
Y	bacterial growth yield (M/M)
ρ	density of water (M/L^3)
v	superficial velocity (L/t)

References

Atkinson B, and Davies IJ. 1974. The overall reaction rate of substrate uptake (reaction) by microbial films. Part I. A biological rate equation. Trans Inst Chem Eng 52:248–259.

Bard Y. 1974. Nonlinear parameter estimation. New York: Academic Press.

Bausum HT, Mitchell WR, Major MA. 1992. Biodegradation of 2,4- and 2,6-dinitrotoluene by freshwater microorganisms. J Environ Sci Health A 27:663–695.

Beck JV, Arnold KJ. 1977. Parameter estimation in engineering and science. New York: John Wiley & Sons.

Blackburn JW, Jain RK, Sayler GS. 1987. Molecular microbial ecology of a napthalene-degrading genotype in activating sludge. Environ Sci Technol 21:884–890.

Blok J. 1994. Extrapolation of biodegradability test data by use of growth kinetic parameters. Ecotoxicol Environ Safety 27:306–315.

Cao YS, Alaerts GJ. 1995. Influence of reactor type and shear stress on aerobic biofilm morphology, population and kinetics. Water Res 29: 107–118.

Characklis WG, Turukhia MH, Zelver N. 1990. Transport and interfacial transfer phenomena. In: Characklis WG, Marshall KC, editors. Biofilms. New York: Wiley. Interscience. New York, NY. p 265–340.

Cheng J, Kanjo Y, Suidan MT, Venosa AD. 1996. Anaerobic biotransformation of 2,4-dinitrotoluene with ethanol as primary substrate: Mutual effect of the substrates on their biotransformation. Water Res 30: 307–314.

Chiu SY, Fan LT, Erickson LE. 1972. Kinetic behavior of mixed populations of activated sludge. Biotechnol Bioeng 14:179–199.

Daigger GT, Grady CPL Jr. 1982. An assessment of the role of physiological adaptation in the transient response of bacterial cultures. Biotechnol Bioeng 24:1427–1444.

Devore JL. 1987. Probability and statistics for engineering and the sciences. Monterey, CA: Brooks/Cole.

Dykhuizen DE, Hartl DL. 1983. Selection in chemostats. Microbiol Rev 47:150–168.

Egli T, Lendenmann U, Snozzi M. 1993. Kinetics of microbial growth with mixtures of carbon sources. Antonie Van Leeuwenhoek 63:289–298.

Grady CPL Jr, Smets BF, Barbeau DS. 1996. Variability in kinetic parameter estimates: A review of possible causes and a proposed terminology. Water Res 30:742–748.

Haigler BE, Nishino SF, Spain JC. 1994. Biodegradation of 4-methyl-5-nitrocatechol by *Pseudomonas* sp. strain DNT. J Bacteriol 176: 3433–3437.

Haigler BE, Suen W-C, Spain JC. 1996. Purification and sequence analysis of 4-methyl-5-nitrocatechol oxygenase from *Burkholderia* sp. strain DNT. J Bacteriol 178:6019–6024.

Hartter DR. 1985. The use and importance of nitroaromatic chemicals in the chemical industry. In: Rickert DE, editor. Toxicity of nitroaromatic compounds. Washington, DC: Hemisphere. p 1–13.

Heath MS, Wirtel SA, Rittmann BE, Noguera DR. 1991. Closure to discussion of: Simplified design of biofilm processes using normalized loading curves 62, 185 (1990). Res J Water Poll Control Fed 63:91–92.

Höfle MG. 1983. Long-term changes in chemostat cultures of *Cytophaga johnsonae.* Appl Environ Microbiol 46:1045–1053.

Holmberg A. 1982. On the practical identifiability of microbial growth models incorporating Michaelis-Menten type non-linearities. Math Biosci 62:23–43.

Jennings PA. 1975. A mathematical model for biological activity in expanded bed adsorption columns. PhD Thesis. University of Illinois, Urbana, IL.

Keith LH, Telliard WA. 1979. Priority pollutants: I. A perspective view. Environ Sci Technol 13:416–423.

Lendenmann U, Egli T. 1998. Kinetic models for the growth of *Escherichia coli* with mixtures of sugars under carbon-limited conditions. Biotechnol Bioeng 59:99–107.

Lendenmann U, Spain JC, Smets BF. 1998. Simultaneous biodegradation of 2,4-dinitrotoluene and 2,6-dinitrotoluene in an aerobic fluidized-bed biofilm reactor. Environ Sci Technol 32:82–87.

Liu D, Thomson K, Anderson AC. 1984. Identification of nitroso compounds from biotransformation of 2,4-dinitrotoluene. Appl Environ Microbiol 47:1295–1298.

Liu Y. 1997. Estimating minimum fixed biomass concentration and active thickness of nitrifying biofilm. J Environ Eng 123:198–202.

Lobry JR, Flandrois JP. 1991. Comparison of estimates of Monod's growth model parameters from the same data set. Binary 3:20–23.

McCormick NG, Cornell JH, Kaplan AM. 1978. Identification of biotransformation products from 2,4-dinitrotoluene. Appl Environ Microbiol 35:945–948.

Neumeier W, Haas R, von Löw E. 1989. Mikrobieller Abbau von Nitroaromaten aus einer ehemaligen Sprengstoffproduktion, Teil 1: Abbau von 2,4,6-trinitrotoluol (TNT). Forum Städte-Hygiene 40:32–37.

Nguyen VT, Shieh WS. 1995. Evaluation of intrinsic and inhibition kinetics of biological fluidized bed reactors. Water Res 29:2520–2524.

Nishino SF, Spain JC. 1996. Degradation of 2,6-dinitrotoluene by bacteria. Presented at the Q-380, Abstracts of the 96th general meeting of the American Society for Microbiology, New Orleans, LA. p 452.

Noguera DR, Freedman DL. 1996. Reduction and acetylation of 2,4-dinitrotoluene by a *Pseudomonas aeruginosa* strain. Appl Environ Microbiol 62:2257–2263.

Popp JA, Leonard TB. 1985. The hepatocarcinogenicity of dinitrotoluenes. In: Rickert DE, editor. Toxicity of nitroaromatic compounds. Washington, DC: Hemisphere. p 53–60.

Rickert DE, Butterworth BE, Popp JA. 1984. Dinitrotoluene: Acute toxicity, oncogenicity, genotoxicity, and metabolism. CRC Crit Rev Toxicol 13:217–234.

Riefler RG, Ahlfeld DP, Smets BF. 1998. Respirometric assay for biofilm kinetics estimation: Parameter identifiability and retrievability. Biotechnol Bioeng 57:35–45.

Rieger P-G, Knackmuss H-J. 1995. Basic knowledge and perspectives on biodegradation of 2,4,6-trinitrotoluene and related nitroaromatic compounds in contaminated soil. In: Spain JC, editor. Biodegradation of nitroaromatic compounds. New York: Plenum Press. p 1–18.

Rittmann BE. 1994. Fundamentals and application of biofilm processes in drinking-water treatment. Quality and treatment of drinking water. In: Hrubec J, editor. The Handbook of environmental chemistry. p 61–87.

Rittmann BE, Crawford L, Tuck CK, Namkung E. 1986. *In situ* determination of kinetic parameters for biofilms: Isolation and characterization of oligotrophic biofilms. Biotechnol Bioeng 28:1753–1760.

Rittmann BE, McCarty PL. 1980. Model of steady-state-biofilm kinetics. Biotechnol Bioeng 22:2343–2357.

Robinson JA, Tiedje JM. 1983. Nonlinear estimation of Monod growth kinetic parameters from a single substrate depletion curve. Appl Environ Microbiol 45:1453–1458.

Rutgers M, Teixeira De Mattos MJ, Postma PW, Van Dam K. 1987. Establishment of steady state in glucose-limited chemostat cultures of *Klebsiella pneumoniae.* J Gen Microbiol 133:445–451.

Sáez PB, Rittmann BE. 1988. An improved pseudo-analytical solution of steady-state biofilms. Biotechnol Bioeng 31:379.

Sáez PB, Rittmann BE. 1990. Error analysis of limiting case solutions of the steady-state biofilm model. Water Res 24:1181–1185.

Schnoor JL. 1996. Environmental modeling: Fate and transport of pollutants in water, air and soil. New York: John Wiley & Sons.

Sen A, Muni S. 1990. Regression analysis: Theory, methods, and applications. New York: Springer.

Shieh WK, Keenan JD. 1986. Fluidized bed biofilm reactor for wastewater treatment. Adv Biochem Eng/Biotechnol 33:131–169.

Sokol W. 1987. Oxidation of an inhibitory substrate by washed cells (oxidation of phenol by *Pseudomonas putida*). Biotechnol Bioeng 30: 921–927.

Sokol W. 1988. Uptake rate of phenol by *Pseudomonas putida* grown in unsteady state. Biotechnol Bioeng 32:1097–1103.

Spain JC. 1995. Biodegradation of nitroaromatic compounds. Ann Rev Microbiol 49:523–555.

Spanggord RJ, Spain JC, Nishino SF, Mortelmans KE. 1991. Biodegradation of 2,4-dinitrotoluene by a *Pseudomonas* sp. Appl Environ Microbiol 57:3200–3205.

Tanyolaç A, Beyenal H. 1996. Predicting average biofilm density of a fully active spherical bioparticle. J Biotechnol 52:39–49.

Van Rolleghem PA, Dochain D, Van Daele M. 1995. Practical identifiability of a biokinetic model of activated sludge respiration. Water Res 29:2561–2570.

Wanner O, Gujer W. 1986. A multispecies biofilm model. Biotechnol Bioeng 28:314–328.

Welty JR, Wicks CE, Wilson RE. 1984. Fundamentals of momentum, heat, and mass transfer. New York: John Wiley & Sons.

Whong W-Z, Edwards GS. 1984. Genotoxic activity of nitroaromatic explosives and related compounds in *Salmonella typhimurium*. Mutat Res 136:209–215.

Williamson K, McCarty PL. 1976. Verification studies of the biofilm model for bacterial substrate utilization. J Water Pollut Control Fed 48:281–296.

Zhang S, Huck PM. 1996. Parameter estimation for biofilm processes in biological water treatment. Water Res 30:456–464.